Published in final edited form as:
J Am Chem Soc. 2013 November 27; 135(47): 17804–17817. doi:10.1021/ja407147d.

Contributions of the S100A9 C-Terminal Tail to High-Affinity Mn(II) Chelation by the Host-Defense Protein Human Calprotectin

Megan Brunjes Brophy, **Toshiki G. Nakashige**, **Aleth Gaillard**, and **Elizabeth M. Nolan***
Department of Chemistry, Massachusetts Institute of Technology, Cambridge, MA 02139

Abstract

Human calprotectin (CP) is an antimicrobial protein that coordinates Mn(II) with high affinity in a Ca(II)-dependent manner at an unusual histidine-rich site (site 2) formed at the S100A8/S100A9 dimer interface. We present a 16-member CP mutant family where mutations in the S100A9 C-terminal tail (residues 96–114) are employed to evaluate the contributions of this region, which houses three histidines and four acidic residues, to Mn(II) coordination at site 2. The results from analytical size-exclusion chromatography, Mn(II) competition titrations, and electron paramagnetic resonance spectroscopy establish that the C-terminal tail is essential for high-affinity Mn(II) coordination by native CP in solution. The studies indicate that His103 and His105 (HXH motif) of the tail complete the Mn(II) coordination sphere in solution, affording an unprecedented biological His_6 site. These solution studies are in agreement with a Mn(II)-CP crystal structure reported recently (*PNAS* **2013**, *110*, 3841). Remarkably high-affinity Mn(II) binding is retained when either H103 or H105 are mutated to Ala, when the HXH motif is shifted from positions 103–105 to 104–106, and when the human tail is substituted by the C-terminal tail of murine S100A9. Nevertheless, antibacterial activity assays employing human CP mutants reveal that the native disposition of His residues is important for conferring growth inhibition against *Escherichia coli* and *Staphylococcus aureus*. Within the S100 family, the S100A8/S100A9 heterooligomer is essential for providing high-affinity Mn(II) binding; the $S100A7_{ox}$, S100A9(C3S), S100A12, and S100B homodimers do not exhibit such Mn(II)-binding capacity.

Introduction

Manganese in microbial pathogenesis is a topic of substantial current interest.[1–21] Human pathogens such as *Borrelia burdgorferi*,[6,7] *Neisseria gonorrhoeae*,[9,10] *Staphylococcus aureus*,[11,12] and *Streptococcus pneumoniae*[13–17] import manganese and employ this metal ion in the oxidative stress response and other processes that include primary metabolism and signal transduction. Recent investigations indicate that Mn(II) acquisition by invading microbial pathogens contributes to virulence and successful colonization in the host.[1] Indeed, a number of bacterial manganese importers (e.g., PsaA, MntH, etc.) are implicated in pathogenesis.[1,17,19,20,22] In the battle against infection, the mammalian host employs diverse defense tactics to prevent microbial replication, one of which is metal-ion withholding.[23–25] The goal of this physiological mechanism is to prevent microbial acquisition of essential nutrient metals that include manganese, iron, and zinc. The antimicrobial host-defense protein calprotectin (CP), the focus of this work, has emerged as a player in the competition between host and pathogen for the transition metal nutrients

*Corresponding author: lnolan@mit.edu, Phone: 617-452-2495, Fax: 617-324-0505.

Supporting Information. Complete Experimental Section including the design of the synthetic genes, Tables S1–S11, Figures S1–S59, and complete ref. 64. These materials are available free of charge via the Internet at http://pubs.acs.org.

Mn(II) and Zn(II).[11,26–31] We seek to decipher the molecular-level details of metal-ion sequestration by CP and thereby acquire a more sophisticated understanding of its contributions to the biology of transition metal ions in multiple contexts, including the host/pathogen interaction.

CP is a member of the S100 protein family.[32–34] S100 family members are ca. 10-kDa Ca(II)-binding polypeptides that form homo- and heterooligomers. Human CP is a heterooligomer of S100A8 (10.8 kDa, α subunit) and S100A9 (13.2 kDa, β subunit), and it exists as a heterodimer (αβ, 24 kDa) or tetramer ($\alpha_2\beta_2$, 48 kDa) (Figure 1A).[35–38] Each S100 subunit contains two Ca(II)-binding EF-hand domains,[39,40] and Ca(II) binding to these sites induces oligomerization of human CP from the dimeric to tetrameric form.[37] Neutrophils, white blood cells that are in circulation and rapidly recruited to sites of infection, express CP in a constitutive manner. At sites of infection, CP is released from neutrophils into the extracelluar space where its concentrations are reported to reach >500 μg/mL.[41] The ability of CP to inhibit microbial growth was first discovered several decades ago,[42–44] and subsequent investigations established that CP exhibits broad-range growth inhibitory action against multiple bacterial and fungal species, the former of which include *Escherichia coli*, *Enterococcus aerogenes*, *Staphylococcus aureus*, *Borrelia burgdorferi*, *Streptococcus pneumoniae*, *Salmonella*, and *Acinetobacter baumannii* amongst others.[11,29,45–47] The antimicrobial action of CP has been attributed to its ability to sequester Zn(II), an essential nutrient for all organisms, in the extracellular space and at sites of infection following cellular release (Figure 1B).[25] More recently, a role for CP in Mn(II) deprivation was highlighted through studies of *Staphylococcus aureus* infection and susceptibility to oxidative killing by neutrophils.[11,48] These seminal investigations demonstrated that CP provided protection against Mn(II) toxicity for a *S. aureus* mutant deficient in the manganese transport regulator MntR and exhibited enhanced antibacterial activity against a mutant lacking the Mn(II) transport proteins MntAB.[11] CP is also proposed to inhibit bacterial invasion of epithelial cells, constituting another host-defense mechanism.[49–51] In addition to infectious disease, CP has been implicated in a range of pathophysiological phenomena that include autoimmunity,[52] inflammation,[53–57] cancer,[58,59] and cardiovascular disease;[60,61] however, the precise details of its contributions to human health and disease, and whether metal ions play a role, are oftentimes unclear.

In support of the metal-chelation-based working model for antimicrobial action, CP houses two transition metal-ion binding sites at the S100A8/S100A9 interface (Figure 1C–F) that have been the subject of several investigations.[38,45,46,48,62] We define sites 1 and 2 as the His_3Asp and His_4/His_6 motifs, respectively.[46] The His_3Asp motif is comprised of (A8)His83, (A8)His87, (A9)His20, and (A9)Asp30, and the interfacial His_4 site arises from (A8)His17, (A8)His27, (A9)His91, and (A9)His95. In prior investigations, we established that sites 1 and 2 each coordinate first-row transition metal ions.[46,62] In particular, both of these sites bind Zn(II) with high affinity and in a Ca(II)-dependent manner.[46] Subsequently, we reported that CP binds only one equivalent of Mn(II) with high affinity at site 2.[62] The Mn(II) affinity of CP is also Ca(II)-dependent, and the Mn(II) dissociation constant (K_d) value of site 2 shifts from the low-micromolar to nanomolar range following Ca(II) complexation (K_{d1} = 4.9 ± 1.0 μM, -Ca(II); K_{d1} = 194 ± 203 nM, +Ca(II); determined by RT-EPR).[62] The nanomolar-range Mn(II) K_d value of CP in the presence of Ca(II) determined by RT-EPR was verified through competition experiments with the fluorescent sensor ZP1 (*vide infra*).[62] The data also suggest that site 1 of Ca(II)-bound CP coordinates Mn(II) with micromolar affinity (K_{d2} = 21 ± 5 μM, RT-EPR).[62] Because Ca(II) ions modulate the transition metal-ion affinities, we proposed a model whereby CP morphs into its high-affinity form when it encounters millimolar concentrations of Ca(II) in the extracellular space.[46] The *in vitro* antibacterial activity of CP is Ca(II)-dependent,

suggesting that the high-affinity heterotetramer is required for potent growth inhibition of both Gram-negative and –positive organisms.[46]

Site 2, defined by four His residues, is an unusual protein-based metal-binding site; the Protein Data Bank (PDB) contains very few examples of native His_4 motifs.[63,64,72,73] Moreover, Mn(II) binding to the histidine-rich site rather than the His_3Asp site is striking given the abundance of coordination environments of known Mn(II)-binding proteins exhibiting mixed N/O donor sets (Table 1). Our reported low-temperature EPR spectroscopic investigations of Mn(II) bound to site 2 are consistent with a nearly-idealized octahedral Mn(II) coordination sphere provided by the four His ligands and two additional ligands of unknown identity.[62] We proposed that the unidentified ligands may be derived from the protein backbone, the C-terminal tail of S100A9 in particular, or solvent molecules. The tail region is disordered in the crystal structure of the CP heterotetramer,[38] and it houses a HHH motif at positions 103–105 and a glutamate at position 111 (Figure 1G). Subsequently, X-ray crystallographic characterization of a Mn(II)-CP complex revealed that the Mn(II) ion coordinated at site 2 is housed in a remarkable octahedral coordination sphere comprised of (A8)His17, (A8)His27, (A9)His91, (A9)His95, (A9)His103, and (A9)His105 (Figure 1F).[45] The latter two residues are located in the S100A9 C-terminal tail. This crystallographic His_6 Mn(II)-binding site is unprecedented in biological systems and suggests an important role for the S100A9 C-terminal tail in metal-ion acquisition and host-defense function. Nevertheless, many details about this unusual Mn(II)-binding site and how the C-terminal tail contributes to the coordination sphere in solution require further elucidation. Herein we present the results of extensive solution-based biochemical and spectroscopic investigations designed to probe this site. Our studies provide critical new insights into site 2, including an evaluation of flexibility in the tail region and how the C-terminal tail contributes to Mn(II) chelation and antibacterial activity. Moreover, we probe the Mn(II)-binding capacities of four other human S100 family members reported to chelate other transition metals (e.g. Zn(II), Cu(II)) and these studies confirm that the S100A8/S100A9 heterooligomer is essential for providing a high-affinity Mn(II) site.

Results and Discussion

Design and Preparation of the Human S100A9 Mutant Family

The C-terminal region of human S100A9 houses four acidic residues (E96, D98, E99, E111) and three His residues (H103, H104, H105). We designed a 16-member S100A9 mutant family to evaluate the contributions of these residues to high-affinity Mn(II) coordination at site 2, which is defined by the interfacial His_4 motif (Table 2). These mutant proteins are based on CP-Ser, which is a heterodimer or –tetramer of S100A8(C42S) and S100A9(C3S) that we have previously employed in metal-binding and antibacterial activity studies.[45,62] The mutant family includes the single mutants E96A, D98A, E99A, H103A, H104A, H105A, K106A, and E111A. The K106A mutant was prepared to probe the consequence of mutating a non-coordinating amino acid in the tail region on Mn(II) complexation. A series of mutants harboring multiple mutations in the C-terminal tail were also designed. CP-Ser-AHA and CP-Ser-AAA allow for further investigation of the contributions of the native HXH motif to Mn(II) coordination. The C-terminal tail of S100A9 contains several glycine residues and is expected to be flexible, and thus CP-Ser-AAA(K106H), CP-Ser-AHA(K106H), and CP-Ser-AAA(L109H)(E111H) were designed to evaluate the importance of His positioning to Mn(II) binding (*vide infra*). CP-Ser-AAE was prepared to probe the consequences of a $N\rightarrow O_x$ (x=1,2) donor substitution on Mn(II) complexation. CP-Ser-Δ101 is a truncation lacking residues 102–114 of S100A9. Lastly, CP-Ser-mT is a chimera of human and mouse S100A9 where the C-terminal 19 residues of human S100A9 are substituted by the C-terminal 17 residues of the mouse congener. The “mouse tail” harbors two HXH motifs at positions 102–104 and 104–106, and a single Cys residue at position 110

(Table 2). Two CP mutant proteins with modifications to the S100A9 C-terminus were reported recently[45] and are analogs of the Δ101 and AAA mutants presented in this work (*vide infra*).

The S100A9 mutant genes were obtained either by site-directed mutagenesis starting from the pET41a-*S100A9(C3S)* template[46] or as synthetic genes from DNA2.0 (Tables S3–S4). The corresponding polypeptides were overexpressed in *E. coli* BL21(DE3) as described previously.[46] Each mutant S100A9 polypeptide was combined with S100A8(C42S) to afford the corresponding heterodimeric CP mutants following purification.[46] Each mutant protein was characterized by SDS-PAGE, mass spectrometry, analytical size-exclusion chromatography (SEC), and circular dichroism (CD) spectroscopy (Figures S1–S27). SDS-PAGE revealed that each CP mutant was obtained in high purity (Figure S1), and mass spectrometry confirmed subunit identity (Table S5). Mass spectrometry revealed that CP-Ser-mT was isolated as the β-mercaptoethanol (BME) adduct that results from disulfide bond formation between (A9)Cys110 and BME (hereafter CP-Ser-mT-BME), the latter of which was employed during the purification to prevent the formation of intermolecular cross-links via (A9)Cys110. A tris(2-carboxyethyl)phosphine (TCEP) reduction protocol was therefore employed to obtain CP-Ser-mT with a free cysteine residue (Experimental Section), and both forms were characterized. The CD spectra of each mutant in the absence and presence of Ca(II) exhibit minima at ca. 208 and 222 nm, establishing that each CP mutant has the expected α-helical fold (Figures S2–S9).[35] Analytical SEC confirmed that each C-terminal tail mutant protein was isolated in the heterodimeric form, and oligomerization to the $\alpha_2\beta_2$ heterotetramers occurred when 2 mM Ca(II) was added to the running buffer as previously observed for CP-Ser (Figures S11–S26, Table S6).[46] In total, biochemical characterization of all members of this mutant family confirms the expected protein behavior and integrity based on prior characterization of CP and metal-binding-site mutants.[46]

The C-Terminal Tail Contributes to Ca(II)-Dependent Oligomerization

Although analytical SEC revealed that CP-Ser-Δ101 (100 μM) and CP-Ser-AAA (100 μM) completely oligomerized to the $\alpha_2\beta_2$ forms when 2 mM of Ca(II) was included in the SEC running buffer, defective Ca(II)-dependent oligomerization was observed when Ca(II) was excluded from the running buffer and each protein (100 μM) was pre-incubated with ≤ 8.0 equiv of Ca(II) (Figure S27). In particular, both CP-Ser-Δ101 and CP-Ser-AAA exhibit defective tetramerization under these conditions relative to CP-Ser.[46] At 8.0 equiv (800 μM) of Ca(II), the SEC traces for Δ101 and AAA exhibit a broad feature comprised of two prominent peaks that roughly correspond to a 1:1 ratio of heterodimer and tetramer eluting from the SEC column. In contrast, CP-Ser exhibits almost complete conversion to the $\alpha_2\beta_2$ heterotetramer when pre-incubated with 8.0 equiv of Ca(II).[46] These observations indicate that deletion or mutation of the S100A9 C-terminal tail impacts the ability of CP to undergo Ca(II)-dependent tetramerization. This point is important from the perspective of employing C-terminal tail truncation or mutant proteins in metal-binding studies because (i) Ca(II) concentrations may affect speciation of mutants differently than for the wild-type protein and (ii) the Mn(II)/Zn(II) affinity of CP is Ca(II) dependent.[46,62]

To ascertain whether truncation or mutation of the C-terminal tail influences the thermal stability of the peptide fold, we employed CD spectroscopy to determine the T_m values for Δ101 and AAA in the absence and presence of 2 mM Ca(II) (Table S7, Figure S10). CP-Ser has a T_m value of ~59 °C that shifts to ~79 °C following Ca(II) binding.[62] CP-Ser-Δ101 and AAA exhibit comparable T_m values under both sets of conditions, indicating that deletion of the tail or mutation of the three His residues has negligible impact on the thermal stability of the heterodimeric and heterotetrameric forms.

Analytical SEC and Thermal Denaturation Studies Support Contribution of the C-Terminal Tail and HHH Motif to Mn(II) Coordination in Solution

We previously reported that Mn(II) coordination to CP (αβ) results in an analytical SEC peak shift to lower elution volume relative to that of the apo heterodimer.[62] CP-Ser αβ elutes at ~11.4 mL (~35.5 kDa), and this peak shifts to ~10.6 mL (~49.5 kDa) following Ca(II)-induced tetramerization whereas Mn(II) coordination to CP-Ser (αβ) affords a SEC peak with an elution volume of ~11.0 mL. We reasoned that the SEC elution volumes of the C-terminal tail mutants (αβ) pre-incubated with excess Mn(II) would provide insight into whether each mutant coordinated Mn(II) and whether Mn(II) remained protein-bound over the course of the elution (Figures 2, S28–S30). The elution behavior of the Mn(II)-treated mutants may be classified into one of three groups. The first group contains mutants that exhibit behavior comparable to that of CP-Ser: E96A, D98A, E99A, H103A, H104A, H105A, K106A, E111A, mT. Each of these mutants exhibits a single, new Mn(II)-dependent peak in the analytical SEC chromatogram characterized by an elution volume that falls between those of the αβ and $\alpha_2\beta_2$ oligomers. We conclude that these mutants all coordinate Mn(II) and, like CP-Ser, retain Mn(II) over the course of the elution. The second group contains mutants that afford chromatograms with broad features defined by two overlapping peaks. These features are observed when the mutants are injected onto the SEC column immediately after Mn(II) addition and following a 2 or 18 h pre-incubation with Mn(II) (Figures S29–S30). The elution volumes of these peaks are within the αβ – $\alpha_2\beta_2$ range, and the peak ratios vary to some degree depending on the mutant. The Δ101, AAA, AAE, AAA(K106H), and AAA(L109H)(E111H) mutants fall into this category, and the chromatograms reveal Mn(II)-dependent formation of new species. We speculate that the two-peak behavior may indicate diminished capacity of these mutants to bind and retain Mn(II) over the course of the SEC elution. The AHA and AHA(K106H) mutants define the third group. The chromatographic behavior of these three mutants is a hybrid of the group 1 and 2 members. A Mn(II)-induced peak shift occurs, but this peak exhibits a prominent tail at higher elution volumes. Again, we reason that these mutants bind Mn(II), but that coordination is perturbed relative to CP-Ser. These SEC experiments were conducted in the absence of Ca(II), and the results report on the ability of CP-Ser (αβ) to bind and retain Mn(II). In prior work, we reported that the Ca(II)-binding EF-hand domains of CP do not coordinate Mn(II) to any appreciable degree and that CP-Ser (αβ) coordinates Mn(II) with low-micromolar affinity.[62] We therefore conclude that the changes in elution volume observed for all CP-Ser tail mutants incubated with Mn(II) indicate that each of these mutants has the capacity to coordinate Mn(II) at site 2 albeit to varying degrees.

To elaborate upon these results, we ascertained whether the presence of Mn(II) perturbs the T_m values for three mutants, Δ101, AAA, and AHA (Table S7, Figure S10). Mn(II) coordination by CP-Ser increases the T_m value for both the αβ and $\alpha_2\beta_2$ oligomers.[62] Because Mn(II) binds at the S100A8/S100A9 interface, we attribute the increased T_m values to Mn(II)-induced stabilization of the heterooligomer. Although an increase in T_m occurs following Mn(II) addition to Δ101, AAA, and AHA, the magnitude of change is small relative to that observed for CP-Ser (Table S7). The T_m value for the Δ101 and AAA heterodimers increases to 65 °C whereas CP-Ser exhibits a T_m of 87 °C in the presence of Mn(II). Likewise, the mutants have T_m values of 88 °C in the presence of both Ca(II) and Mn(II) compared to >95 °C for CP-Ser. Although deletion of the tail or mutation of its three His residues has no impact on the thermal stability of the apo and Ca(II)-bound scaffolds, the Mn(II)-bound mutants exhibit reduced thermal stability relative to CP-Ser. This trend further supports the notion that the C-terminal tail and HHH motif are important for Mn(II) complexation.

Mn(II)-Binding Titrations by ZP1 Competition and RT-EPR Confirm a Role for the C-Terminal Tail

With support for Mn(II) complexation by the C-terminal tail mutants from SEC, we evaluated the relative Mn(II) affinities through a series of Mn(II) competition titrations employing the fluorescent metal-ion sensor ZP1. ZP1 is a calcium-insensitive turn-on Zn(II) sensor with relatively high background fluorescence (Φ = 0.38 at pH 7.0).[74] ZP1 also coordinates Mn(II) (K_{d1} = 550 nM, K_{d2} = 2.2 μM),[75] and this metal ion quenches ZP1 emission. In prior work, we took advantage of the Ca(II) insensitivity and Mn(II)-induced turn-off of ZP1 to probe the Mn(II) affinities of CP-Ser and the metal-binding site mutants CP-Ser ΔHis_3Asp, ΔHis_4, and $\Delta\Delta$ (Table S1).[62] Although we were unable to obtain quantitative K_d values from the CP-Ser/ZP1 competitions because ZP1 outcompeted CP-Ser $\alpha\beta$ (low Mn(II) affinity form) and CP-Ser $\alpha_2\beta_2$ (high Mn(II) affinity form) outcompeted ZP1 under the experimental conditions, these titrations provide a reliable readout of relative Mn(II) affinities. Thus, we performed Mn(II) competition assays with ZP1 and the C-terminal tail mutant proteins in the presence of 50-fold excess Ca(II), which we expect to provide full conversion of CP to the heterotetrameric form. In addition to providing a relative measure of Mn(II) affinities, the results also facilitate identification of the protein-based residues required for high-affinity Mn(II) coordination in solution.

Figure 3 exhibits the Mn(II) competition results for CP-Ser and a selection of C-terminal tail mutant proteins, and individual plots for all mutants are provided as Supporting Information (Figures S31–S36). In this assay, enhanced competition between ZP1 and a CP mutant protein ($\alpha_2\beta_2$) relative to CP-Ser ($\alpha_2\beta_2$) indicates that the mutant exhibits reduced Mn(II) affinity. The Mn(II) competition trends establish a number of important facets related to Mn(II) coordination by CP: (i) the E96A, D98A, E99A, K106A and E111A mutants exhibit behavior comparable to CP-Ser ($\alpha_2\beta_2$) and outcompete ZP1 for Mn(II). None of the acidic residues in the C-terminal region of S100A9 are essential for high-affinity Mn(II) chelation by CP-Ser, as suggested by analytical SEC. (ii) CP-Ser-Δ101 and AAA afford the greatest competition with ZP1 for Mn(II). The titration curves for these mutants are similar to those reported for CP-Ser(H91A), CP-Ser(H95A) and CP-Ser(H27D),[62] and indicate that deletion of the C-terminal tail or removal of the HHH motif decreases the Mn(II) affinity but does not completely preclude Mn(II) binding. (iii) The titration curves for the H103A, H104A, H105A, and AHA mutants fall between those of CP-Ser and CP-Ser-AAA and provide a relative Mn(II) affinity ordering of CP-Ser ~ H104A > H103A ~ H105A > AHA > AAA. The H104A and CP-Ser titration curves are virtually superimposable up to 0.75 equiv of Mn(II)/CP added. (iv) Movement of the HXH motif from positions 103–105 to 104–106 and 109–111 allows ZP1 to more readily compete for Mn(II) and indicates a Mn(II) affinity ordering of CP-Ser > CP-Ser-AHA(K106H) > CP-Ser-AAA(L109H)(E111H). Likewise, the AAE mutant readily competes with ZP1 for Mn(II); its titration curve is most similar to those of Δ101 and AAA. In total, the ZP1 competition experiments support the necessity of the HXH motif and specifically H103 and H105 as key contributors for high-affinity Mn(II) binding at site 2. These studies also indicate that flexibility in the C-terminal tail allows for H104 or non-native His residues to contribute to Mn(II) binding in the absence of the native HXH motif. In particular, the titrations suggest that H104 participates in the absence of H103 and H105, and that His residues placed at distant locales (i.e. $\geq$ position 106) can modulate the Mn(II) affinity relative to Δ101 and AAA.

Both the analytical SEC and ZP1 competition experiments indicate that Δ101 and AAA coordinate Mn(II) with relatively weak affinity at site 2 in both the absence (SEC experiments) and presence (ZP1 experiments) of Ca(II). These results are in disagreement with a recent ITC study where negligible enthalpy change was observed following titration of either HN Tail (AAA analog, His$\rightarrow$Asn mutations) or ΔTail (Δ101 analog) with Mn(II)

and was attributed to no binding (K_d = NB).[45] To further probe the Mn(II) binding ability of these mutants, we performed room-temperature EPR titrations to determine whether Mn(II) addition to CP-Ser-Δ101 and AAA affords an attenuated free Mn(II) signal. The EPR spectrum of free Mn(II) (e.g. $[Mn(H_2O)_6]^{2+}$) exhibits a six-line pattern at g = 2 (a = 8.9 mT) at room temperature that results from hyperfine splitting (I = 5/2) of the allowed EPR transition ($\Delta m_s = 1$, $\Delta m_I = 0$) in high-spin S = 5/2 ^{55}Mn(II) systems.[76,77] In contrast, protein-bound Mn(II) is EPR silent at room temperature because the zero-field splittings broaden the signal beyond detection.[78,79] For both CP-Ser-Δ101 and AAA, plots of $[Mn_{free}]$ / CP versus $[Mn_{total}]$ / CP provided slopes in the 0.7–0.8 range, indicating an attenuation in the free Mn(II) signal that results from Mn(II) binding (Table S8, Figure S37). In prior work, we obtained similar slopes RT-EPR titrations of CP-Ser (αβ) mutants lacking one His residue at the His_4 site.[62] Based on the analytical SEC, ZP1 and RT-EPR experiments, we conclude that Δ101 and AAA are able to coordinate Mn(II) at site 2 in both the absence and presence of Ca(II), albeit with lower affinity than CP-Ser. The precise origins for the discrepancy between these investigations and the conclusions drawn from ITC titrations are unclear; however, ITC directly measures the enthalpic contribution to binding equilibria and entropy driven metal-binding events are not detectable by this method.[80] Moreover, the Ca(II) ion concentration employed in the ITC studies was described as stoichiometric,[45] and the speciation of CP/mutant (αβ versus $\alpha_2\beta_2$) in these studies is ambiguous. We previously reported that an excess of Ca(II) (>20 equiv) is required for CP-Ser to fully sequester Mn(II) from ZP1[62] and we report defective Ca(II)-induced tetramerization for the Δ101 and AAA mutants in this work.

Low-Temperature EPR Spectroscopy Supports the Contribution of the HXH Motif

Simulation of the low-temperature EPR spectrum obtained for CP-Ser ($\alpha_2\beta_2$) in the presence of substoichiometric Mn(II) afforded zero-field splitting parameters consistent with a nearly idealized octahedral coordination environment (D = 270 MHz, E/D = 0.30).[62] To further probe the Mn(II) coordination sphere, we determined whether this Mn(II) EPR signal is retained for the C-terminal tail mutants. We acquired the EPR spectra for samples containing 100-μM mutant protein in the presence of 0.3 equiv Mn(II) and in the absence or presence of 10 equiv of Ca(II) (Figure 4, S38–S40). Figure 4A displays the low-temperature Mn(II) EPR spectra for the Ca(II)-bound forms of CP-Ser, E96A, D98A, E99A, E111A, and Δ101. The EPR signals for E96A, D98A, E99A, and E111A are characterized by a six-line pattern centered at g = 2, and the features and intensities are comparable to those of CP-Ser ($\alpha_2\beta_2$). In contrast, a dramatic loss of signal intensity and definition at g = 2 occurs for Δ101. This signal is comparable to the Mn(II) signals previously reported for the His_4 single mutants (A8)H17A, (A8)H27A, (A9)H91A, and (A9)H95A.[62] Moreover, the spectra for CP-Ser-AAA and CP-Ser-AHA closely resemble that of Δ101, as do the spectra for the H103A and H105A single mutants (Figure 4B). In contrast, the Mn(II) EPR signal of H104A is indistinguishable from that of CP-Ser. These data further demonstrate that CP utilizes the S100A9 C-terminal tail to coordinate Mn(II) in solution, and demonstrate the importance of H103 and H105 for Mn(II) binding. In total, the results of our biochemical and spectroscopic investigations support an octahedral coordination sphere comprised of (A8)His17, (A8)His27, (A9)His91, (A9)His95, (A9)His103, and (A9)His105. This assignment is in agreement with a recent X-ray crystal structure of the Mn(II)-CP complex (Figures 1,5)[45] and indicates that CP employs a hexahistidine coordination sphere for Mn(II) at site 2 in both solution and the solid state. Thermodynamic and spectroscopic solution studies such as the ones presented in this work are essential for elucidating whether a coordination mode identified by X-ray crystallography also occurs in solution and hence under more physiologically-relevant conditions.

Comparisons of the Mn(II) EPR signatures obtained for the mutant proteins E96A, D98A, E99A, H104A, K106H, and E111A in the absence and presence of Ca(II) reveal increases in the intensities of the Mn(II)-CP EPR signals and sharpening of both the allowed and semi-forbidden transitions in the presence of excess Ca(II) (Figures S38–S40). Ca(II)-induced sharpening of the transitions is also observed for CP-Ser-AHA(K106H) and CP-Ser-AAA(L109H)(E111H), and the human-mouse chimera (*vide infra*). This behavior was previously reported for CP-Ser and was attributed to formation of higher-affinity Mn(II) complexes in the Ca(II)-bound forms.[62]

The Mn(II) competition experiments (*vide supra*) indicate that the H103A and H105A heterotetramers coordinate Mn(II) with sufficient affinity to outcompete ZP1 for the metal ion (Figure 3); however, mutation of either H103 or H105 results in loss of the six-coordinate Mn(II) EPR signal characteristic of CP-Ser (Figure 4). One possible explanation for these observations is that the H103A and H105A mutants form high-affinity five-coordinate Mn(II) species that are not observable by low-temperature EPR at the sample concentrations employed in this study. Further spectroscopic and structural studies are required to address this notion.

The S100A9 HXH Motif Is Conserved

Amino acid sequence alignment of human S100A9 with S100A9s from other organisms reveals a conserved HXH motif in the C-terminal tail region (Figure 6). Whereas bovine and rabbit S100A9 exhibit a single HXH motif, murine and rat S100A9s contain two adjacent HXH motifs (i.e. HXHXH). To probe whether CP variants harboring S100A9 chimeras retain high-affinity Mn(II) coordination, we prepared and characterized CP-Ser-mT (Table 1 and Supporting Information). This mutant is a chimera of human and mouse S100A9 where the C-terminal 19 residues of human S100A9 are substituted by the C-terminal 17 residues of the mouse congener. CP-Ser-mT contains a single Cys at position 110 and it was isolated as a Cys110-BME adduct. This adduct was reduced with TCEP and the resulting protein was buffer exchanged into argon- or nitrogen-purged buffer to remove the BME adduct and prevent undesirable cysteine-based oligomerization. The Mn(II)-binding properties of both CP-Ser-mT and CP-Ser-mT-BME were investigated. The chimeras coordinate Mn(II) with high affinity (Figure S36), and we observed no evidence for participation of Cys110. Moreover, the low-temperature EPR signal of 100 μM CP-Ser-mT incubated with 30 μM Mn(II) exhibit features that are identical to those of CP-Ser ($\alpha_2\beta_2$) both in the absence and presence of Ca(II) (Figure S40). It is noteworthy that the Mn(II) signal for CP-Ser-mT ($\alpha\beta$) exhibits considerably greater intensity and definition compared to that of CP-Ser ($\alpha\beta$), but is less intense than for CP-Ser-mT ($\alpha_2\beta_2$). One possible explanation for these subtle differences is that CP-Ser-mT ($\alpha\beta$) coordinates a larger proportion of Mn(II) in a six-coordinate manner compared to CP-Ser ($\alpha\beta$). Alternatively, the CP-Ser-mT sample may contain less free Mn(II) in solution, and thus the signal resulting from six-coordinate Mn(II)-bound CP-Ser-mT is undistorted. In total, biochemical and spectroscopic studies of CP-Ser-mT support the notion that His residues within the mouse tail are necessary for high-affinity Mn(II) coordination. Because the mouse tail harbors two adjacent HXH motifs, the identities of the His residues presumed to contribute to Mn(II) binding at site 2 are currently unclear. Moreover, the fact that CP-Ser-mT ($\alpha_2\beta_2$) retains the ability to coordinate Mn(II) with high affinity, and exhibits a CP-Ser-like EPR spectroscopic signature, indicates that the precise amino acid sequence of the tail region is dispensable at least to some degree. Nevertheless, the amino acid sequence of the tail region may have as-yet unappreciated contributions to metal-ion coordination at site 2, as evidenced by the EPR signatures of CP-Ser-mT, and the heterooligomeric properties of calprotectin homologs, which are largely unexplored, may also influence metal-ion coordination. Further biophysical and structural investigations are

required to evaluate the contributions of tail composition and oligomerization state to the coordination sphere and metal-ion affinity at site 2 for various CP congeners.

Magnesium(II) Does Not Confer CP Tetramerization or High-Affinity Mn(II) Binding

EF-hand domains can coordinate Mg(II) in addition to Ca(II), and various physiological roles for Mg(II) binding have been proposed.[39] In this regard, EF-hand domains may be classified as "calcium-specific" or "calcium/magnesium" sites depending on the Mg(II) affinities.[39] To the best of our knowledge, no studies supporting Mg(II) complexation by CP have been reported to date. We questioned whether Mg(II) modulates the Mn(II) affinity of human CP as does Ca(II). Thus, we investigated the oligomerization and Mn(II)-binding ability of CP-Ser (αβ) in the presence of excess Mg(II) (Figures S41–S43). Analytical SEC revealed no change in the elution volume of CP-Ser (αβ) when either 2 or 10 mM Mg(II) was included in the running buffer, demonstrating that excess Mg(II) does not promote tetramerization of CP-Ser. We confirmed that the Mn(II) turn-off response of ZP1 is Mg(II)-insensitive, and Mn(II) competition experiments established that ZP1 outcompetes CP-Ser for Mn(II) in the presence of 2 or 10 mM Mg(II). Overnight incubations of ZP1, CP-Ser, Mn(II), and Mg(II) provided the same result. We conclude that the Ca(II)-induced tetramerization and modulation of Mn(II)-binding affinity is Ca(II)-specific and not generalizable to Mg(II) and likely other alkaline earth metals.

Contributions of Site 2 and the C-Terminal Tail to Antibacterial Action

The broad-range antibacterial and antifungal activities of CP are well established.[11,29,45–47] We previously reported that wild-type CP and CP-Ser exhibit indistinguishable and Ca(II)-dependent antibacterial activity against several Gram-negative and –positive species, and that only one metal-binding site is necessary for bacterial growth inhibition on a short timescale (t = 8 h).[46] In contrast, we observed that the CP-Ser ΔHis_4 mutant exhibited attenuated activity against both *E. coli* and *S. aureus* relative to CP-Ser and CP-Ser ΔHis_3Asp (t = 20 h). We reasoned that this behavior may either point to an important role of the His_4 site in host defense or arise from comprised protein integrity of the mutant.[46] Subsequently, attenuated growth inhibitory activity of a ΔHis_4 mutant was observed for additional bacterial species including the human pathogens *Acinetobacter baumannii, Pseudomonas aeruginosa*, and *Staphylococcus* spp.[45]

Thus, we first sought an independent method to probe the ramifications of blocking site 2 on antimicrobial action. We pre-incubated CP-Ser ($\alpha_2\beta_2$) or ΔHis_3Asp ($\alpha_2\beta_2$) with 1.0 equiv of Mn(II) to occupy site 2 and employed the resulting Mn(II)-bound forms in antibacterial activity assays (Figure 7). Whereas apo ΔHis_3Asp exhibited antibacterial activity similar to that of CP-Ser, Mn(II)-bound ΔHis_3Asp was inactive against both *E. coli* ATCC 25922 and *S. aureus* ATCC 25923. Moreover, Mn(II)-bound CP-Ser and ΔHis_4 displayed comparable growth inhibitory activity. In both cases, this activity is attenuated relative to CP-Ser and ca. 50% growth inhibition is observed in the presence of 1.0 mg/mL CP. The observation that Mn(II)-bound CP-Ser exhibits the same activity profile as ΔHis_4 suggests that the attenuated activity observed by this mutant does not result from mutation of the CP sequence compromising protein integrity.

We next aimed to probe how mutations in the S100A9 C-terminal tail influence antibacterial activity and we evaluated the growth inhibitory capacity of select C-terminal tail mutants, H104A, E111A, AAA, AHA, and AHA(K106H), against both *E. coli* and *S. aureus* (Figure 7). We selected these mutants to probe the consequences of (i) deleting the native Mn(II) ligands (AAA, AHA), (ii) including other His residues that provide high-affinity Mn(II) complexation judging by the ZP1 competitions (AHA, AHA(K106H), and (iii) alterations to non-coordinating residues of the tail region (H104A, E111A). The H104A and E111A

single-point mutants exhibited antibacterial activity comparable to that of CP-Ser, demonstrating that mutation of a non-coordinating His or Glu residue in the tail does not perturb the ability of CP-Ser to inhibit bacterial growth under these assay conditions. In contrast, antibacterial activity was attenuated for AAA, AHA, and AHA(K106H) relative to CP-Ser. These mutants retain the ability to coordinate Mn(II), albeit with lower affinity, and exhibited activity profiles comparable to those of ΔHis_4 and Mn(II)-bound CP-Ser. The AAA result is in general agreement with a recent study of the HN Tail mutant.[45] In total, these investigations demonstrate that both metal-binding sites contribute to the antibacterial activity of CP; however, the contributions of each site differ, and these *in vitro* assays suggest that the contributions of each site are not synergistic. Perturbation of site 2 has much more pronounced impact on growth inhibition than complete loss of site 1.

Other Human S100 Proteins Do Not Coordinate Mn(II) with High Affinity

The human S100 protein family contains 21 polypeptides, and a number of the members coordinate first-row transition metal ions at interfacial sites (e.g. CP, A7, A12, B) [38,72,81,82] or at undefined locales (e.g., murine A9)[83] (Figures S45–S48). CP is unique amongst the transition-metal-binding S100s because it is a heterooligomer, and this composition gives rise to two different metal-binding sites. Site 2 is unusual amongst S100s because it is comprised of four His residues as a result of His27 of S100A8. This residue aligns with Asp residues in other S100 proteins (Figure 1). S100B provides one other example of a His_4 site, which was identified following crystallization of $Zn(II)_2$:S100B at pH 9.72 Moreover, S100A9 is the only polypeptide of this class to exhibit a C-terminal extension, making CP and the S100A9 homodimer the only two family members to exhibit C-terminal tails.

To the best of our knowledge, no other S100 protein has been reported to bind Mn(II) and participate in Mn(II) homeostasis. One ITC study of S100A12 afforded negligible enthalpy change with Mn(II) addition, but no other solution-based metal-binding studies were performed to ascertain whether this result indicates a lack of Mn(II) complexation.[45] The remarkable structural features of CP that make it stand alone in the S100 family are key contributors to the Mn(II)-binding site, which indicates that high-affinity Mn(II) chelation may be a property unique to CP. To test this notion, case-by-case analysis of the metal-binding properties other S100 family members is required, and we overexpressed and purified the human forms of $S100A7_{ox}$, S100A9(C3S), S100A12, and S100B (Figures S49–S52). In the apo forms, these S100s are antiparallel homodimers. S100A7, S100A12, and S100B each exhibit two metal-chelating His_3Asp (S100A7, S100A12), His_3Glu (S100B), or His_4 (S100B) sites at the dimer interface (Figures S45, S47, and S48). The crystal structure of human S100A9 reveals no well-defined metal-binding sites at the homodimer interface (Figure S46);[84] however, ^{65}Zn-labeling studies indicated that murine S100A9 binds Zn(II), and that a mutant lacking the C-terminal tail retained less radiolabel compared to wild-type.[83] We evaluated Mn(II)-binding ability of each S100 protein by analytical SEC, ZP1 competition titrations, and EPR spectroscopy in both the absence and presence of excess Ca(II) (Figures S53–S55). We found no evidence for high-affinity Mn(II) coordination by $S100A7_{ox}$, S100A9(C3S), S100A12, or S100B. $S100A7_{ox}$ may bind manganese with weak affinity. Although $S100A7_{ox}$ did not compete with ZP1 for Mn(II), the analytical SEC chromatogram of $S100A7_{ox}$ pre-incubated with 10 equiv of Mn(II) exhibited a peak with a pronounced tail (Figure S53) and the low-temperature EPR spectrum of $S100A7_{ox}$ in the presence of 0.3 equiv of Mn(II) revealed a Mn(II) signal with extremely weak intensity (Figure S55). We attempted to further probe Mn(II)-binding by $S100A7_{ox}$ using room-temperature EPR and observed a distorted Mn(II) signal of lower intensity than the Mn(II) atomic absorption standard at substoichiometric equivalents of Mn(II). Although it is unlikely that S100A7 binds Mn(II) with sufficient affinity to sequester the metal in a biological context, further studies of this metal/protein interaction are warranted. To confirm

that the purified homodimers were isolated in the apo forms, and that the lack of observable Mn(II) complexation did not result from other metal ions (i.e. zinc) blocking the binding sites, the metal/S100 ratios were quantified by either inductively-coupled plasma mass spectrometry (ICP-MS) or inductively coupled plasma optical emission spectrometry and these ratios provided no evidence for significant metal-ion contamination (Table S11). Based on these investigations, we conclude that the high-affinity Mn(II)-binding capacity of CP is unique and a consequence of its heterooligomeric structure.

Summary and Perspectives

CP provides a remarkable strategy for how to sequester labile Mn(II) in biological systems. In this work, we employ biochemical and spectroscopic techniques to interrogate the unusual histidine-rich Mn(II)-coordination site of human CP, in addition to Mn(II) binding by related S100 proteins. Our solution studies are in excellent agreement with recent crystallographic studies of a Mn(II)-CP complex (Figure 1D and 1F).[45] Moreover, investigations of the H103A, H104A, H105A, and AHA mutants provide fundamental insights into the contributions of the native HHH motif to Mn(II) binding and antibacterial action, and other tail mutants such as AHA(K106H), AAA(L109H)(E111H), and the human-mouse chimera allow evaluation of the importance of His positioning within the flexible tail region. In addition to revealing the hexahistidine motif for Mn(II) chelation at site 2 in the solid state, the crystallographic coordinates deposited in the PDB (PDB 4GGF) indicate 50% occupancy of site 1 with Mn(II) in three of the four heterodimers in the asymmetric unit (Figure 1D). The fourth heterodimer exhibits no electron density corresponding to a Mn(II) ion in site 1 and (A9)Asp30 is rotated away from the metal-binding site. The Mn(II) ion housed in site 1 is five coordinate with (A8)His83, (A8)H9s87, (A9)His20 and bidentate (A9)Asp30 providing a N_3O_2 motif. Although the Mn(II) ion housed in the unprecedented His_6 motif has received the most attention,[45] the partial occupancy of Mn(II) in site 1 is noteworthy and consistent with Mn(II)-binding titrations of CP-Ser conducted by room-temperature EPR.[62] In this study, a second binding event (K_{d2} = 21 ± 5 μM) was required to fit the RT-EPR titration curve when the sample included excess Ca(II), and we tentatively assigned K_{d2} to weak Mn(II) complexation to the His_3Asp site.[62] Thus, given this crystallographic insight, it will be informative to identify spectroscopic signals for Mn(II) coordinated to the His_3Asp site in future work. The Mn(II)-CP X-ray crystal structure also reveals a hydrogen-bonding interaction between His95 and Asp98 (Figure S56). It is possible that this hydrogen-bonding interaction affords an imidizolate-like ligand at His95 and creates a site with a formal charge of 1+ and thereby contributes to the high Mn(II) affinity in addition to providing a mechanism of charge neutralization. Asp98, however, is not conserved (Figure 6), and characterization of the D98A mutant did not reveal a diminished affinity for Mn(II), at least by the methods employed in this work. We also note that substitution of H27 or H105 with anionic ligands (e.g. H27D[62], AAE) does not afford high-affinity Mn(II) binding. Why CP employs six neutral ligands to coordinate Mn(II) and the mechanism for balancing the charge conferred by the Mn(II) ion are currently unclear and require further investigation.

Both the Ca(II)-modulated Mn(II) affinities and hexahistidine Mn(II) coordination motif exhibited by CP are unprecedented in known biological systems. Other characterized manganese-binding proteins, including enzymes and transporters, employ mixed oxygen- and nitrogen-donor atoms for chelating this metal ion (Table 1). Hexaimidazole coordination motifs are also rare in small-molecule Mn(II) coordination chemistry. Of greater than 640,000 small-molecule structures deposited in the Cambridge Structural Database (CSD),[85] there are ca. 330 structures of mononuclear complexes containing Mn(II) coordinated by six nitrogen-donor ligands. Of these structures, we identified six compounds with hexaimidazole motifs.[86–91] These complexes exhibit Mn(II) ligated by either unsubstituted

or *N*-substituted imidazoles, and the Mn—N bond lengths span the 2.16 to 2.37 Å range. For example, hexakis(imidazole) manganese(II) dichloride tetrahydrate, $\{[Mn(C_3H_4N_2)_6]Cl_2 \bullet 4H_2O\}$,86 exhibits Mn—N bond lengths of ca. 2.27 Å, and the Mn(II) complex $\{[Mn(TMIMA)_2](PF_6)_2\}$ (TMIMA, tris[1-methyl-2-imidazolyl)methyl]amine) has Mn(II)–N bond distances ranging from 2.307 to 2.366 Å.[89] The CSD also includes multinuclear Mn(II) complexes defined by hexaimidazole motifs,[92,93] including a trinuclear complex with imidazolyl ligands bridging octahedral and tetrahedral Mn(II) centers displaying Mn(II)–N bond distances of 2.246 to 2.313 Å at the octahedral site.[93] For Mn(II)-CP, the Mn(II)–N bond distances of site 2 vary from 2.18 to 2.37 Å, which is within the range defined by such small-molecule analogs.

The C-terminal region of S100A9 has been implicated in a potpourri of biophysical and biological phenomena. Yeast two-hybrid studies of S100A8/S100A9 interactions indicated a role for the S100A9 C-terminal tail in heterooligomerization.[94] Subsequently, CP lacking the S100A9 C-terminal tail was observed to exhibit slightly attenuated antifungal activity against *Candida albicans*, leading to the proposal that the tail may contribute to CP-mediated Zn(II) sequestration.[95,96] Investigations of homodimeric murine S100A9 revealed retention of ^{65}Zn(II) that was dependent on the presence of the C-terminal region.[82] The tail region has also been implicated in arachidonic acid binding by CP,[97] which is reported to be zinc-reversible,[98] and as a modulator of adherent peritoneal cell function (murine S100A9).[99,100] In accord with recent crystallographic studies,[45] the current work supports an additional role for the C-terminal tail in Mn(II) complexation and its contributions to antimicrobial activity.

Like CP, several other proteins, and predominantly those used for metal-ion transport, employ flexible regions for metal-ion coordination. The extracellular N-terminal region of the eukaryotic copper transporter Ctr1 contains metal-binding residues that are utilized to coordinate bioavailable copper. *In vitro* studies with synthetic model peptides indicated that human Ctr1 employs a combination of Met and His residues to bind Cu(I) and Cu(II) with high affinities whereas yeast Crt1 utilizes a series of MXXXM and MXM motifs to bind Cu(I).[101–103] The bacterial Zn(II) transporter ZnuA contains one N_3O_1 site for high-affinity Zn(II) coordination.[104] ZnuA also contains a flexible region that is rich in His, Glu, and Asp residues; this region contributes to the formation of a low-affinity Zn(II) binding site of unknown function.[104,105] The nickel metallochaperones UreE and SlyD contain C-terminal histidine-rich motifs that coordinate Ni(II) *in vitro*.[106–108] To the best of our knowledge, CP provides a unique example of a Mn(II)-binding protein harboring a flexible tail that encapsulates the metal ion. Indeed, coordination of Mn(II) by the two histidine residues in the C-terminal tail allows CP to trap labile Mn(II) in the biological milieu. It will be important to determine whether the C-terminal tail also contributes to Zn(II) coordination at site 2.

The antibacterial activity assays presented in this work reveal that H103 and H105 are essential for CP to provide its full *in vitro* growth-inhibitory ability against select Gram-negative and –positive organisms (Figure 7). Site 1 and 2 thus contribute to this biological function differently. Previous evaluation of the antibacterial activity of a ΔHis_4 mutant against a range of bacterial species, in addition to studies of the activities of ΔTail and HN Tail mutants against *S. aureus*, also demonstrated that site 2 has a greater contribution to growth-inhibitory function than site 1, and this outcome was attributed to Mn(II) deprivation for all organisms.[45] The possibility of a general Mn(II)-dependent mechanism of CP action is intriguing; however, CP is multifaceted and understanding the precise molecular-level origins for the site-dependent antimicrobial activity of CP will require further investigations at the molecular and organismal levels. In particular, elucidating M(II)-CP speciation in a variety of biological contexts is necessary as well as considering the mechanism of CP

action against susceptible microorganisms on a case-by-case basis. Calprotectin coordinates both Zn(II) and Mn(II) with high affinity, and microbial deprivation of either metal ion has deleterious consequences. From the standpoint of Zn(II) homeostasis, the antibacterial activity assay results for the ΔHis_4 and C-terminal tail mutants are striking because site 1 binds Zn(II) with picomolar affinity in both CP and the ΔHis_4 mutant.[46] Various studies have suggested a role for Zn(II) chelation by CP in the host/pathogen interaction,[25–31,96] and we expect Zn(II) deprivation to be deleterious for laboratory strains (e.g. *E. coli* ATCC 25922). From the perspective of Mn(II) and the work described here, CP-Ser-AHA and AHA(K106H) ($\alpha_2\beta_2$) both outcompete ZP1 for Mn(II), which supports formation of high-affinity Mn(II) complexes, yet the antibacterial activity of each mutant is attenuated relative to CP-Ser. This observation implies that high-affinity Mn(II) coordination does not directly correlate with growth inhibition; however, we note that these mutants may not coordinate Mn(II) with sufficiently high affinity to outcompete bacterial Mn(II) transporters and the metal-binding equilibria established in the ZP1 competitions and in a bacterial growth assay differ substantially. Moreover, the relative rates of metal-ion dissociation from CP must also be considered in the context of the working model (Figure 1B). Our prior studies revealed a relatively slow rate of Mn(II) dissociation from site 2.[62] It is possible that Mn(II) dissociates from CP more readily in the absence of the native HXH motif and, by corollary, Zn(II) may also dissociate more readily if the HXH motif is also involved in Zn(II) coordination or if deletion/mutation of the tail perturbs Zn(II) binding at site 2 in another manner. A greater rate of M(II) dissociation means that the metal ion is not effectively sequestered and thus may confer attenuated growth inhibitory action because the dissociated metal ion can be acquired by microbial transport machinery.

Manganese is important for the virulence of many pathogens, and yet little is known about how the host transports and stores manganese in addition to how it prevents manganese uptake by pathogens at both the physiological and molecular levels. Biochemical and spectroscopic studies of CP provide essential new insights into this phenomenon and inform biological work. The results presented here support a model in which the S100A9 C-terminal tail of CP encapsulates Mn(II), providing a high-affinity binding site and preventing its release. This mechanism of metal-ion capture is consistent with the proposed physiological function of CP as a metal-sequestering protein that inhibits microbial acquisition of these essential nutrients, and provides a working model for how CP captures labile Mn(II) in the biological milieu.

Supplementary Material

Refer to Web version on PubMed Central for supplementary material.

Acknowledgments

The Searle Scholars Program (Kinship Foundation), the MIT Center for Environmental Health Sciences (NIH P30-ES002109), and the MIT Department of Chemistry are gratefully acknowledged for financial support. We thank Dr. Ralph Weber, Dr. Jeffrey Simpson, and Alexandria Liang for assistance with the EPR spectrometer located in the MIT Department of Chemistry Instrumentation Facility; Debby Pheasant for assistance with the CD spectrometer; Sumin Kim for preparing the pET41a-*S100A7* plasmid; Professors Christopher T. Walsh and JoAnne Stubbe for insightful discussions. The circular dichroism spectrometer is housed in the MIT Biophysical Instrumentation Facility for the Study of Complex Macromolecular Systems, which is supported by grants NSF 0070319 and NIH GM68762.

References

1. Papp-Wallace KM, Maguire ME. Annu Rev Microbiol. 2006; 60:187–209. [PubMed: 16704341]
2. Zaharik ML, Finlay BB. Frontiers Biosci. 2004; 9:1035–1042.
3. Kehres DG, Maguire ME. FEMS Microbiol Rev. 2003; 27:263–290. [PubMed: 12829271]

4. Jakubovics NS, Jenkinson HF. Microbiology. 2001; 147:1709–1718. [PubMed: 11429449]
5. Stubbe J, Cotruvo JA Jr. Curr Opin Chem Biol. 2011; 15:284–290. [PubMed: 21216656]
6. Aguirre JD, Clark HM, McIlvin M, Vazquez C, Palmere SL, Grab DJ, Seshu J, Hart PJ, Saito M, Culotta VC. J Biol Chem. 2013; 288:8468–8478. [PubMed: 23376276]
7. Esteve-Gassent MD, Elliott NL, Seshu J. Mol Microbiol. 2009; 71:594–612. [PubMed: 19040638]
8. Veyrier FJ, Boneca IG, Cellier MF, Taha MK. Plos Pathogens. 2011; 7:e1002261. [PubMed: 21980287]
9. Tseng HJ, Srikhanta Y, McEwan AG, Jennings MP. Mol Microbiol. 2001; 40:1175–1186. [PubMed: 11401721]
10. Wu HJ, Seib KL, Srikhanta YN, Edwards J, Kidd SP, Maguire TL, Hamilton A, Pan KT, Hsiao HH, Yao CW, Grimmond SM, Apicella MA, McEwan AG, Wang AHJ, Jennings MP. J Proteomics. 2010; 73:899–916. [PubMed: 20004262]
11. Corbin BD, Seeley EH, Raab A, Feldmann J, Miller MR, Torres VJ, Anderson KL, Dattilo BM, Dunman PM, Gerads R, Caprioli RM, Nacken W, Chazin WJ, Skaar EP. Science. 2008; 319:962–965. [PubMed: 18276893]
12. Débarbouillé M, Dramsi S, Dussurget O, Nahori MA, Vaganay E, Jouvion G, Cozzone A, Msadek T, Duclos B. J Bacteriol. 2009; 191:4070–4081. [PubMed: 19395491]
13. Jacobsen FE, Kazmierczak KM, Lisher JP, Winkler ME, Giedroc DP. Metallomics. 2011; 3:38–41. [PubMed: 21275153]
14. Ogunniyi AD, Mahdi LK, Jennings MP, McEwan AG, McDevitt CA, Van der Hoek MB, Bagley CJ, Hoffmann P, Gould KA, Paton JC. J Bacteriol. 2010; 192:4489–4497. [PubMed: 20601473]
15. Jakubovics NS, Valentine RA. Mol Microbiol. 2009; 72:1–4. [PubMed: 19226325]
16. Johnston JW, Briles DE, Myers LE, Hollingshead SK. Infect Immun. 2006; 74(2):1171–1180. [PubMed: 16428766]
17. Johnston JW, Myers LE, Ochs MH, Benjamin WH Jr, Briles DE, Hollingshead SK. Infect Immun. 2004; 72:5858–5867. [PubMed: 15385487]
18. Abrantes MC, Kok J, Lopes MdF. Infec Immun. 2013; 81:935–944. [PubMed: 23297382]
19. Anderson ES, Paulley JT, Gaines JM, Valderas MW, Martin DW, Menscher E, Brown TD, Burns CS, Roop RM II. Infect Immun. 2009; 77:3466–3474. [PubMed: 19487482]
20. Boyer E, Bergevin I, Malo D, Gros P, Cellier MFM. Infect Immun. 2002; 70:6032–6042. [PubMed: 12379679]
21. Kehres DG, Zaharik ML, Finlay BB, Maguire ME. Mol Microbiol. 2000; 36:1085–1100. [PubMed: 10844693]
22. Schreur PJW, Rebel JMJ, Smits MA, van Putten JPM, Smith HE. J Bacteriol. 2011; 193:5073–5080. [PubMed: 21784944]
23. Weinberg ED. JAMA. 1975; 231:39–41. [PubMed: 1243565]
24. Kehl-Fie TE, Skaar EP. Curr Opin Chem Biol. 2009; 14:218–224. [PubMed: 20015678]
25. Hood MI, Skaar EP. Nat Rev Microbiol. 2012; 10:525–537. [PubMed: 22796883]
26. Sohnle PG, Collins-Lech C, Wiessner JH. J Infect Dis. 1991; 164(1):137–142. [PubMed: 2056200]
27. Loomans HJ, Hahn BL, Li QQ, Phadnis SH, Sohnle PG. J Infect Dis. 1998; 177:812–814. [PubMed: 9498472]
28. Lulloff SJ, Hahn BL, Sohnle PG. J Lab Clin Med. 2004; 144:208–214. [PubMed: 15514589]
29. Liu JZ, Jellbauer S, Poe AJ, Ton V, Pesciaroli M, Kehl-Fie TE, Restrepo NA, Hosking MP, Edwards RA, Battistoni A, Pasquali P, Lane TE, Chazin WJ, Vogl T, Roth J, Skaar EP, Raffatellu M. Cell Host Microbe. 2012; 11:227–239. [PubMed: 22423963]
30. Hood MI, Mortensen BL, Moore JL, Zhang Y, Kehl-Fie TE, Sugitani N, Chazin WJ, Caprioli RM, Skaar EP. Plos Pathogens. 2012; 8:e1003068. [PubMed: 23236280]
31. Clohessy PA, Golden BE. Scand J Immunol. 1995; 42:551–556. [PubMed: 7481561]
32. Zimmer DB, Eubanks JO, Ramakrishnan D, Criscitiello MF. Cell Calcium. 2013; 53:170–179. [PubMed: 23246155]
33. Fritz G, Botelho HM, Morozova-Roche LA, Gomes CM. FEBS J. 2010; 277:4578–4590. [PubMed: 20977662]

34. Gross, SR.; Sin, CGT.; Barraclough, R.; Rudland, PS. Cell Mol Life Sci. ASAP; 2013.
35. Hunter MJ, Chazin WJ. J Biol Chem. 1998; 273:12427–12435. [PubMed: 9575199]
36. Leukert N, Sorg C, Roth J. Biol Chem. 2005; 386:429–434. [PubMed: 15927886]
37. Leukert N, Vogl T, Strupat K, Reichelt R, Sorg C, Roth J. J Mol Biol. 2006; 359:961–972. [PubMed: 16690079]
38. Körndorfer IP, Brueckner F, Skerra A. J Mol Biol. 2007; 370:887–898. [PubMed: 17553524]
39. Gifford JL, Walsh MP, Vogel HJ. Biochem J. 2007; 405:199–221. [PubMed: 17590154]
40. Chazin WJ. Acc Chem Res. 2011; 44:171–179. [PubMed: 21314091]
41. Johne B, Fagerhol MK, Lyberg T, Prydz H, Brandtzaeg P, Naess-Andresen CF, Dale I. J Clin Pathol: Mol Pathol. 1997; 50:113–123.
42. Mcnamara MP, Wiessner JH, Collinslech C, Hahn BL, Sohnle PG. Lancet. 1988; 2:1163–1165. [PubMed: 2903377]
43. Sohnle PG, Collinslech C, Wiessner JH. J Infect Dis. 1991; 163:187–192. [PubMed: 1984467]
44. Steinbakk M, Naessandresen CF, Lingaas E, Dale I, Brandtzaeg P, Fagerhol MK. Lancet. 1990; 336:763–765. [PubMed: 1976144]
45. Damo SM, Kehl-Fie TE, Sugitani N, Holt ME, Rathi S, Murphy WJ, Zhang YF, Betz C, Hench L, Fritz G, Skaar EP, Chazin WJ. Proc Natl Acad Sci U S A. 2013; 110:3841–3846. [PubMed: 23431180]
46. Brophy MB, Hayden JA, Nolan EM. J Am Chem Soc. 2012; 134:18089–18100. [PubMed: 23082970]
47. Lusitani D, Malawista SE, Montgomery RR. Infect Immun. 2003; 71:4711–4716. [PubMed: 12874352]
48. Kehl-Fie TE, Chitayat S, Hood MI, Damo S, Restrepo N, Garcia C, Munro KA, Chazin WJ, Skaar EP. Cell Host Microbe. 2011; 10:158–164. [PubMed: 21843872]
49. Nisapakultorn K, Ross KF, Herzberg MC. Infect Immun. 2001; 69:3692–3696. [PubMed: 11349032]
50. Zaia AA, Sappington KJ, Nisapakultorn K, Chazin WJ, Dietrich EA, Ross KF, Herzberg MC. Mucosal Immunol. 2009; 2:43–53. [PubMed: 19079333]
51. Sorenson BS, Khammanivong A, Guenther BD, Ross KF, Herzberg MC. Mucosal Immunol. 2011; 5:66–75. [PubMed: 22031183]
52. Loser K, Vogl T, Voskort M, Lueken A, Kupas V, Nacken W, Klenner L, Kuhn A, Foell D, Sorokin L, Luger TA, Roth J, Beissert S. Nat Med. 2010; 16:713–718. [PubMed: 20473308]
53. Kerkhoff C, Voss A, Scholzen TE, Averill MM, Zanker KS, Bornfeldt KE. Exp Derm. 2012; 21:822–826. [PubMed: 22882537]
54. Střiž I, Trebichavský I. Physiol Res. 2004; 53:245–253. [PubMed: 15209531]
55. Golden BE, Clohessy PA, Russell G, Fagerhol MK. Arch Dis Child. 1996; 74:136–139. [PubMed: 8660076]
56. Vogl T, Tenbrock K, Ludwig S, Leukert N, Ehrhardt C, van Zoelen MAD, Nacken W, Foell D, van der Poll T, Sorg C, Roth J. Nat Med. 2007; 13:1042–1049. [PubMed: 17767165]
57. Goyette J, Geczy CL. Amino Acids. 2011; 41:821–842. [PubMed: 20213444]
58. Lukanidin E, Sleeman JP. Sem Cancer Biol. 2012; 22:216–225.
59. Nakatani Y, Yamazaki M, Chazin WJ, Yui S. Mediat Inflamm. 2005:280–292.
60. Averill MM, Kerkhoff C, Bornfeldt KE. Arterioscl Throm Vas Biol. 2012; 32:223–229.
61. McCormick MM, Rahimi F, Bobryshev YV, Gaus K, Zreiqat H, Cai H, Lord RSA, Geczy CL. J Biol Chem. 2005; 280:41521–41529. [PubMed: 16216873]
62. Hayden JA, Brophy MB, Cunden LS, Nolan EM. J Am Chem Soc. 2013; 135:775–787. [PubMed: 23276281]
63. Arnoux B, Gaucher JF, Ducruix A, Reiss-Husson F. Acta Crystallogr D. 1995; 51:368–379. [PubMed: 15299304]
64. Jaroszewski L, et al. Proteins. 2004; 56:611–614. [PubMed: 15229893]
65. Anand R, Dorrestein PC, Kinsland C, Begley TP, Ealick SE. Biochemistry. 2002; 41:7659–7669. [PubMed: 12056897]

66. Vogt M, Lahiri S, Hoogstraten CG, Britt RD, DeRose VJ. J Am Chem Soc. 2006; 128:16764–16770. [PubMed: 17177426]
67. Greenleaf WB, Jefferson J, Perry P, Hearn AS, Cabelli DE, Lepock JR, Stroupe ME, Tainer JA, Nick HS, Silverman DN. Biochemistry. 2004; 43:7038–7045. [PubMed: 15170341]
68. Lee YH, Deka RK, Norgard MV, Radolf JD, Hasemann CA. Nat Struc Biol. 1999; 6:628–633.
69. Tottey S, Waldron KJ, Firbank SJ, Reale B, Bessant C, Sato K, Cheek TR, Gray J, Banfield MJ, Dennison C, Robinson NJ. Nature. 2008; 455:1138–1142. [PubMed: 18948958]
70. Rukhman V, Anati R, Melamed-Frank M, Adir N. J Mol Biol. 2005; 348:961–969. [PubMed: 15843026]
71. McDevitt CA, Ogunniyi AD, Valkov E, Lawrence MC, Kobe B, McEwan AG, Paton JC. PloS Pathog. 2011; 7:e1002357. [PubMed: 22072971]
72. Ostendorp T, Diez J, Heizmann CW, Fritz G. Biochim Biophys Acta. 2011; 1813:1083–1091. [PubMed: 20950652]
73. Silvennoinen L, Sandalova T, Schneider G. FEBS Lett. 2009; 583:2917–2921. [PubMed: 19665022]
74. Walkup GK, Burdette SC, Lippard SJ, Tsien RY. J Am Chem Soc. 2000; 122:5644–5645.
75. You Y, Tomat E, Hwang K, Atanasijevic T, Nam W, Jasanoff AP, Lippard SJ. Chem Commun. 2010; 46:4139–4141.
76. Stich TA, Lahiri S, Yeagle G, Dicus M, Brynda M, Gunn A, Aznar C, DeRose VJ, Britt RD. App Magn Reson. 2007; 31:321–341.
77. Reed GH, Poyner RR. Met Ions Biol Sys. 2000; 37:183–207.
78. Reed GH, Cohn M. J Biol Chem. 1970; 245:662–664. [PubMed: 4312870]
79. Hunsicker-Wang L, Vogt M, DeRose VJ. Meth Enz. 2009; 468:335–367.
80. Grossoehme NE, Spuches AM, Wilcox DE. J Biol Inorg Chem. 2010; 15:1183–1191. [PubMed: 20725755]
81. Moroz OV, Blagova EV, Wilkinson AJ, Wilson KS, Bronstein IB. J Mol Biol. 2009; 391:536–551. [PubMed: 19501594]
82. Brodersen DE, Nyborg J, Kjeldgaard M. Biochemistry. 1999; 38:1695–1704. [PubMed: 10026247]
83. Raftery MJ, Collinson L, Geczy CL. Protein Expres Purif. 1999; 15:228–235.
84. Itou H, Yao M, Fujita I, Watanabe N, Suzuki M, Nishihira J, Tanaka I. J Mol Biol. 2002; 316:265–276. [PubMed: 11851337]
85. Allen FH. Acta Cryst. 2002; B58:380–388.
86. Garrett TPJ, Guss JM, Freeman HC. Acta Cryst C. 1983; 39:1027–1031.
87. Dev S, Ramli E, Rauchfuss TB, Wilson SR. Inorg Chem. 1991; 30:2514–2519.
88. Niu SY, Zhang SS, Li XM, Wen YH, Jiao K. Acta Cryst E. 2004; 60:M209–M211.
89. Durot S, Policar C, Cisnetti F, Lambert F, Renault JP, Pelosi G, Blain G, Korri-Youssoufi H, Mahy JP. Eur J Inorg Chem. 2005:3513–3523.
90. Lemoine P, Viossat V, Dayan E, Dung NH, Viossat B. Inorg Chim Acta. 2006; 359:4274–4280.
91. Dong GY, Liu TF, He CH, Deng XC, Shi XG. Acta Cryst E. 2011; 67:M960–U1283.
92. Li JH, Nie JJ, Xu DJ. Acta Crystallogr E. 2008; 64:M1108–U118.
93. Lehnert R, Seel F. Z Anorg Allg Chem. 1980; 464:187–194.
94. Propper C, Huang XH, Roth J, Sorg C, Nacken WG. J Biol Chem. 1999; 274:183–188. [PubMed: 9867828]
95. Sohnle PG, Hunter MJ, Hahn B, Chazin WJ. J Infect Dis. 2000; 182:1272–1275. [PubMed: 10979933]
96. The possibility of Mn(II) chelation as an antimicrobial mechanism was not considered in early studies and prior to publication of ref. 11.
97. Sopalla C, Leukert N, Sorg C, Kerkhoff C. Biol Chem. 2002; 383:1895–1905. [PubMed: 12553726]
98. Kerkhoff C, Vogl T, Nacken W, Sopalla C, Sorg C. FEBS Lett. 1999; 460:134–138. [PubMed: 10571075]

99. Pagano RL, Sampaio SC, Juliano L, Juliano MA, Giorgi R. Inflamm Res. 2005; 54:204–210. [PubMed: 15953992]

100. Pagano RL, Sampaio SC, Juliano MA, Juliano L, Giorgi R. Eur J Pharm. 2009; 628:240–246.

101. Jiang J, Nadas IA, Kim MA, Franz KJ. Inorg Chem. 2005; 44:9787–9794. [PubMed: 16363848]

102. Rubino JT, Riggs-Gelasco P, Franz KJ. J Biol Inorg Chem. 2010; 15:1033–1049. [PubMed: 20437064]

103. Haas KL, Putterman AB, White DR, Thiele DJ, Franz KJ. J Am Chem Soc. 2011; 133:4427–4437. [PubMed: 21375246]

104. Yatsunyk LA, Easton JA, Kim LR, Sugarbaker SA, Bennett B, Breece RM, Vorontsov II, Tierney DL, Crowder MW, Rosenzweig AC. J Biol Inorg Chem. 2008; 13:271–288. [PubMed: 18027003]

105. Castelli S, Stella L, Petrarca P, Battistoni A, Desideri A, Falconi M. Biochem Biophys Res Commun. 2013; 430:769–773. [PubMed: 23206707]

106. Won HS, Lee BJ. J Biochem. 2004; 136:635–641. [PubMed: 15632303]

107. Song HK, Mulrooney SB, Huber R, Hausinger RP. J Biol Chem. 2001; 276:49359–49364. [PubMed: 11591723]

108. Kaluarachchi H, Altenstein M, Sugumar SR, Balbach J, Zamble DB, Haupt C. J Mol Biol. 2012; 417:28–35. [PubMed: 22310044]

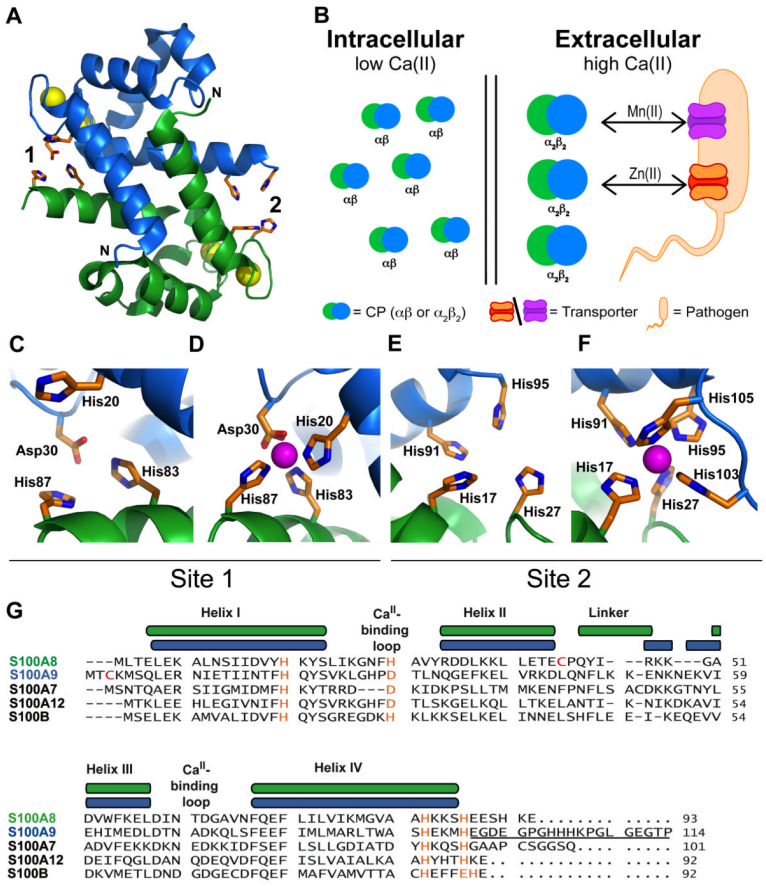

Figure 1.

Structural features of human CP and proposed mechanism of antimicrobial activity. (A) Model of the CP αβ heterodimer, which is taken from the structure of the Ca(II)-bound tetramer (PDB: 1XK4) (ref 38). S100A8 is shown in green, and S100A9 is shown in blue. The Ca(II) ions are depicted as yellow spheres, and transition metal-ion binding residues are presented as orange sticks. No structure of the Ca(II)-free heterodimer is available. (B) Proposed mechanism of antimicrobial action. CP is stored in cells primarily as the apo αβ heterodimer. CP is released at sites of infection where it undergoes Ca(II)-dependent oligomerization to the $\alpha_2\beta_2$ tetramer and competes with pathogens for Mn(II) and Zn(II). (C) Site 1, the His_3Asp motif, is formed at the dimer interface by (A8)His83, (A8)His87, (A9)His20, and (A9)Asp30 PDB: 1XK4). (D) The Mn(II)-His_3Asp site of human CP. The Mn(II) ion, depicted as a magenta sphere, was refined with an occupancy of 0.5 (PDB: 4GGF). (E) Site 2, the His_4 motif, is formed at the dimer interface by (A8)His17, (A8)His27, (A9)His91, and (A9)His95 (PDB: 1XK4). (F) The Mn(II)-His_6 site; the Mn(II) coordination sphere at site 2 is completed by (A9)His103 and (A9)His105. The Mn(II) ion is depicted as a magenta sphere (PDB: 4GGF) (ref 45). (G) Sequence alignment of S100A8 and S100A9 with S100A7, S100A12, and S100B. The secondary structural elements of S100A8 and S100A9 are color-coded and shown above the alignment. Cysteine residues mutated to serine for metal-binding studies are red, and transition metal-binding residues are orange. The C-terminal tail of S100A9 is underlined.

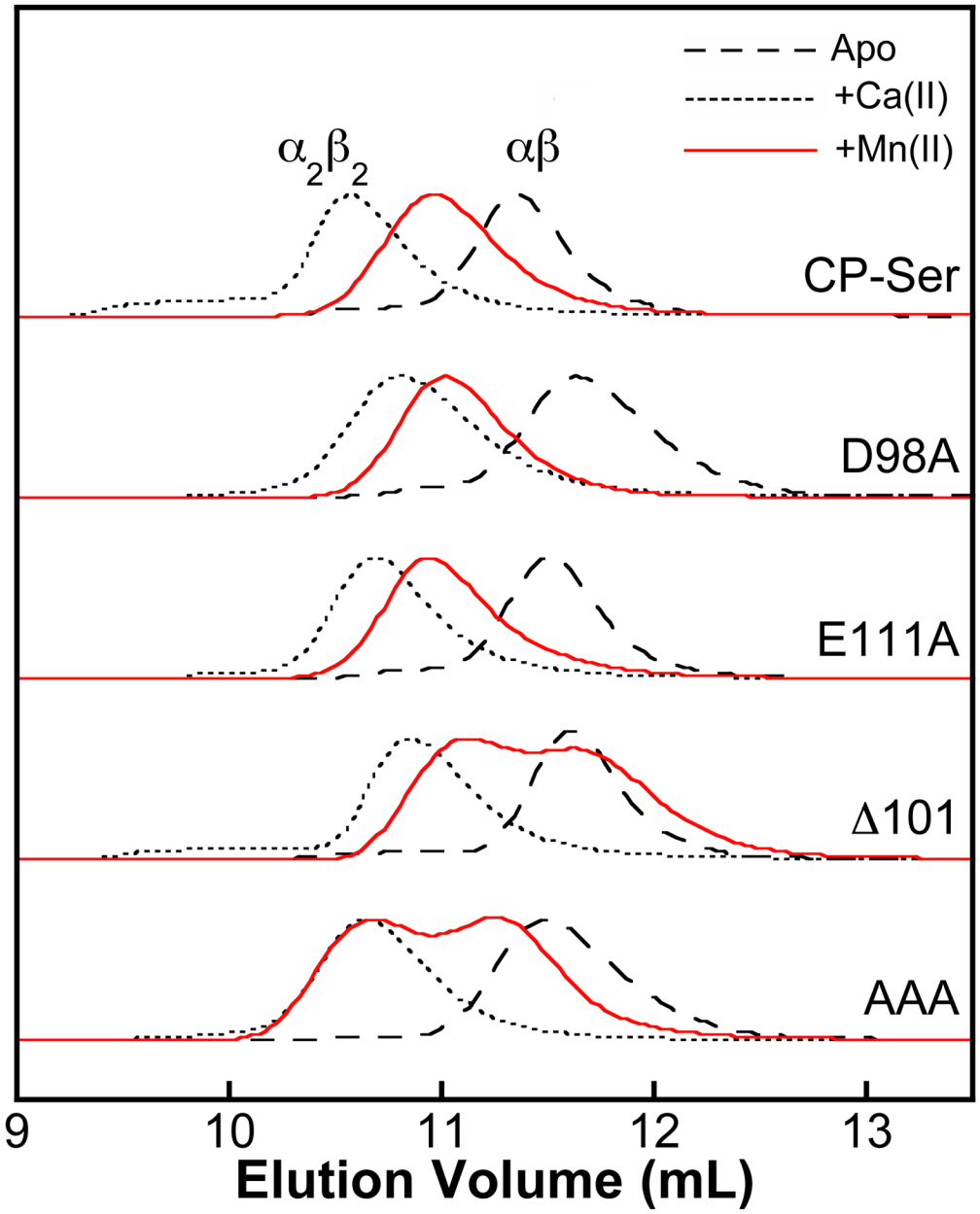

Figure 2.

Analytical SEC of CP-Ser and mutant proteins in the absence and presence of 10 equiv of Mn(II) (75 mM HEPES, 100 mM NaCl, pH 7.5). The proteins were pre-incubated with 10 equiv of Mn(II) (solid red line). The chromatograms for each protein in the absence (dashed line, $\alpha\beta$) and presence (dotted line, $\alpha_2\beta_2$) of 2 mM Ca(II) in the SEC running buffer are provided as standards. The protein concentrations were 200 μM with Mn(II) and 100 μM with and without Ca(II). The chromatograms were normalized to maximum peak absorbance values of 1. Additional Mn(II) SEC chromatograms are provided in Figures S28–S30.

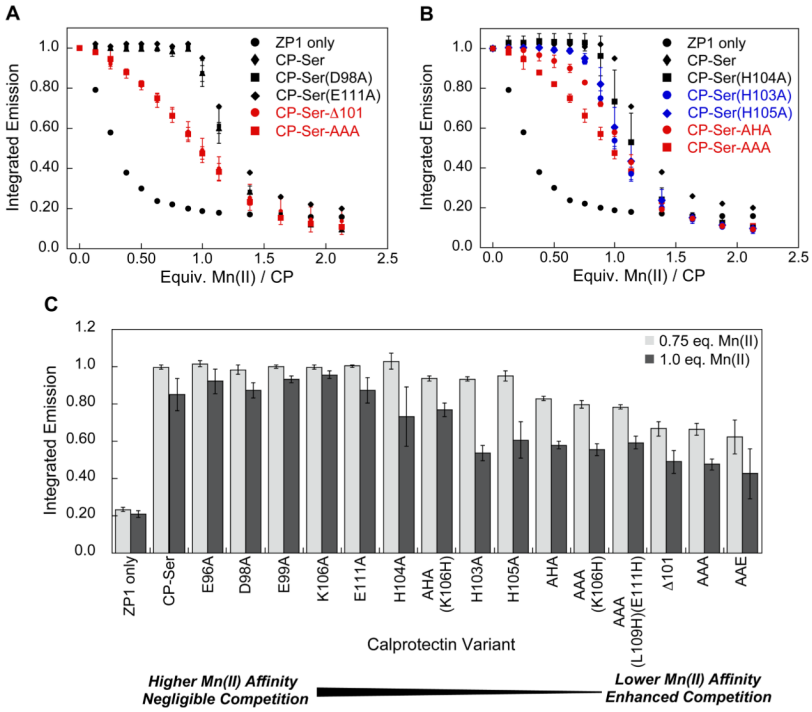

Figure 3.

Select S100A9 C-terminal tail mutants compete with ZP1 for Mn(II) (75 mM HEPES, 100 mM NaCl, pH 7.0). (A) Δ101 and AAA compete with ZP1 for Mn(II), whereas the D98A and E111A exhibit behavior similar to CP-Ser. (B) Mutants of the HHH sequence compete with ZP1 for Mn(II). In panels A and B, one representative titration for ZP1 only and CP-Ser are shown. (C) Integrated ZP1 emission in the presence of 4 μM CP and 200 μM Ca(II) with 3 (light gray, 0.75 equiv) or 4 (dark gray, 1.0 equiv) μM Mn(II). ZP1 is the no-protein control. The data are normalized to apo ZP1 emission. All error bars represent the standard deviation from the mean (n = 3). Additional Mn(II) competition titrations are provided in Figures S31–S36.

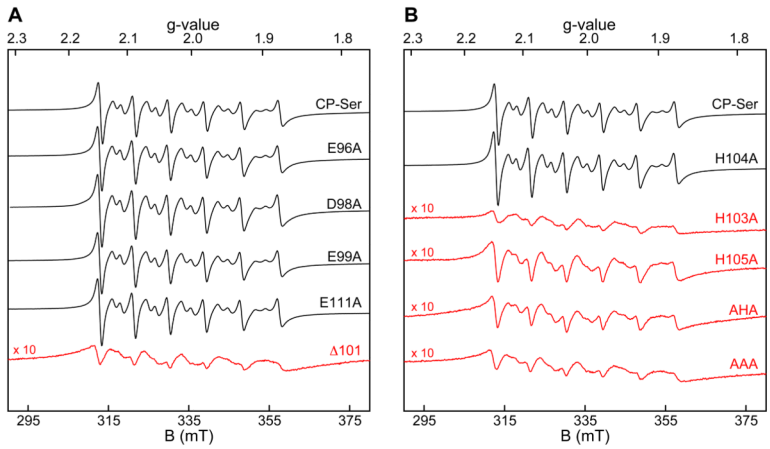

Figure 4.

Low-temperature EPR spectra of CP C-terminal tail mutants (75 mM HEPES, 100 mM NaCl, pH 7.5). (A) Low-temperature EPR signals of CP-Ser, E96A, D98A, E99A, E111A, and Δ101. The Δ101 spectrum is scaled by 10×. (B) Low-temperature EPR spectra of CP-Ser, H104A, H103A, H105A, AHA, and AAA. The H103A, H105A, AHA, and AAA spectra are all scaled by 10×. All samples contain 100 μM protein, 1 mM Ca(II), and 30 μM Mn(II). Instrument conditions: temperature, 20 K; microwaves, 0.2 mW at 9.4 GHz; modulation amplitude, 0.5 mT. Additional EPR spectra are provided in Figures S38–S40.

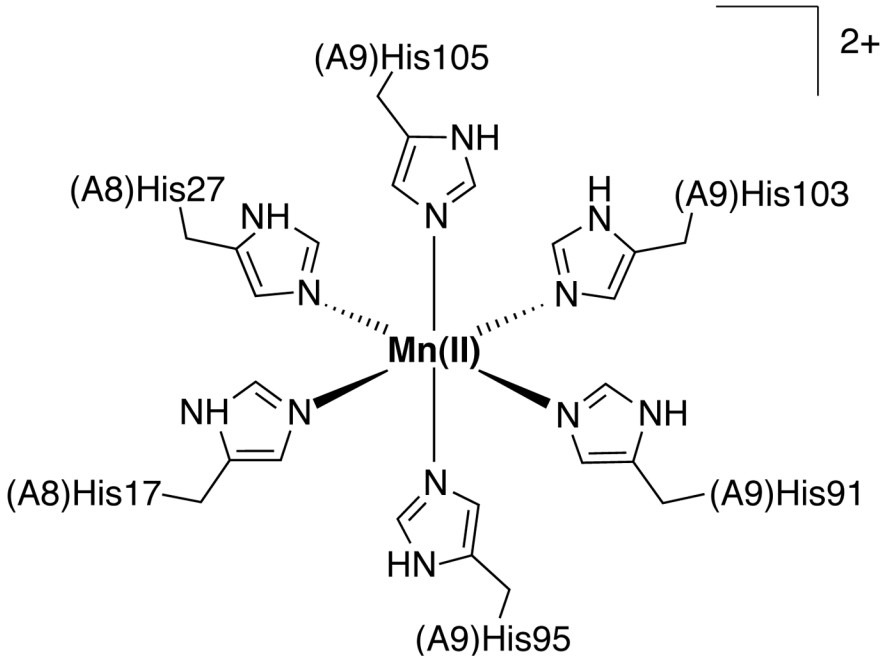

Figure 5.
The Mn(II) coordination sphere at site 2 of human CP, as supported by crystallographic[45] and solution studies. Mn(II) is coordinated in an octahedral manner by (A8)His17, (A8)His27, (A9)His91, (A9)His95, (A9)His103 and (A9)His105.

Figure 6.

Sequence alignment of the C-terminal regions of various S100A9 homologs. The C-terminal HXH motif (underlined) is conserved among S100A9 proteins from multiple species. The alignment of the full protein sequences is provided in Figure S44.

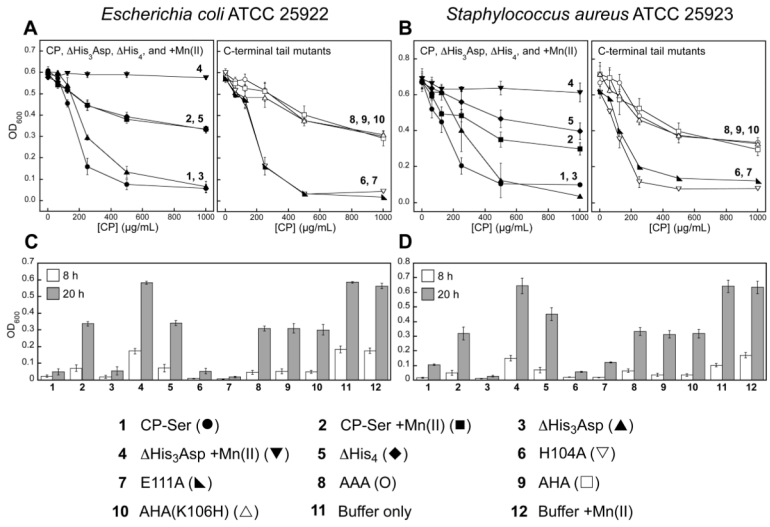

Figure 7.

Antimicrobial activity of CP-Ser and metal-binding-site mutants against *E. coli* ATCC 25922 (A and C) and *S. aureus* ATCC 25923 (B and D). Bacterial cultures were treated with CP-Ser (**1**, ●), CP-Ser pre-incubated with 1.0 equiv Mn(II) (**2**, ■), ΔHis_3Asp (**3**, ▲), ΔHis_3Asp pre-incubated with 1.0 equiv Mn(II) (**4**, ▼), ΔHis_4 (**5**, ◆), (H104A) (**6**, ▽), (E111A) (**7**, ◣), AAA (**8**, ○), AHA (**9**, □), and AHA(K106H) (**10**, △). Control experiments with untreated buffer only (**11**) and buffer with a 42-μM Mn(II) supplement (**12**) were also performed. (A and B) The OD_{600} values were recorded at t = 20 h (mean ± SEM, n = 6). For clarity, the metal-binding-site mutant and Mn(II) pre-incubation assay results are shown in the left panels, and the C-terminal tail mutant assay results are shown in the right panels. (C and D) The cultures were incubated with 1.0 mg/mL protein, and OD_{600} values were recorded at t = 8 and 20 h (mean ± SEM, n = 6).

Table 1

Mononuclear Mn(II)-coordination Motifs Found in Biological Systems.

Protein	Species	CN[a]	Motif	Coordinating Groups	Ref
CP Site 2	*H. sapiens*	6	N_6	His17, His27, His91, His95, His103, His105	45, this work
PRC[b]	*R. spaeroides*	6	N_4O_2	His190, His219, His230, His266, Glu234	63
TM1459	*T. maritima*	6	N_4O_2	His52, His54, His58, His92, H_2O, H_2O	64
OXDC[c]	*B. subtilis*	6	N_3O_3	His273, His275, His319, Glu280, H_2O, H_2O	65
HHRz[d]	N/A (viruses)	6	N_1O_5	Guanine10, $PO_4R_2^{1-}$, H_2O, H_2O, H_2O, H_2O	66
CP Site 1	*H. sapiens*	5	N_3O_2	His20, Asp30, His83, His87	45
MnSOD	*H. sapiens*	5	N_3O_2	His26, His74, His163, Asp159, H_2O	67
TroA[e]	*T. pallidum*	5	N_3O_2	His68, His133, His199, Asp279	68
MncA	*Synechocystis* 6803	5	N_3O_2	His101, His103, His147, Glu108, H_2O	69
MntC	*Synechocystis* 6803	5	N_2O_3	His89, His154, Glu220, Asp295	70
PsaA	*S. pneumoniae*	4	N_2O_2	His67, His138, Glu205, Asp280	71

[a] Coordination number.

[b] Photochemical reaction center.

[c] Oxalate decarboxylase.

[d] Hammer-head ribozyme.

[e] TroA was crystallized with Zn(II).

Table 2

Amino Acid Sequences of the C-terminal Tail of CP-Ser and Mutants.[a]

Protein[b]	Sequence[c,d,e]
CP-Ser	A9(1-90)-HEKMHEGDEG PGHHHKPGLG EGTP
CP-Ser-Δ101	A9(1-90)-HEKMHEGDEG P
CP-Ser-mT	A9(1-90)-HEKMH*ENNPR GHGHSHGKGC GK*
CP-Ser(E96A)	A9(1-90)-HEKMHAGDEG PGHHHKPGLG EGTP
CP-Ser(D98A)	A9(1-90)-HEKMHEGAEG PGHHHKPGLG EGTP
CP-Ser(E99A)	A9(1-90)-HEKMHEGDAG PGHHHKPGLG EGTP
CP-Ser(H103A)	A9(1-90)-HEKMHEGDEG PGAHHKPGLG EGTP
CP-Ser(H104A)	A9(1-90)-HEKMHEGDEG PGHAHKPGLG EGTP
CP-Ser(H105A)	A9(1-90)-HEKMHEGDEG PGHHAKPGLG EGTP
CP-Ser(K106A)	A9(1-90)-HEKMHEGDEG PGHHHAPGLG EGTP
CP-Ser(E111A)	A9(1-90)-HEKMHEGDEG PGHHHKPGLG AGTP
CP-Ser-AHA	A9(1-90)-HEKMHEGDEG PGAHAKPGLG EGTP
CP-Ser-AAA	A9(1-90)-HEKMHEGDEG PGAAAKPGLG EGTP
CP-Ser-AAE	A9(1-90)-HEKMHEGDEG PGAAEKPGLG EGTP
CP-Ser-AAA(K106H)	A9(1-90)-HEKMHEGDEG PGAAAHPGLG EGTP
CP-Ser-AHA(K106H)	A9(1-90)-HEKMHEGDEG PGAHAHPGLG EGTP
CP-Ser-AAA(L109H)(E111H)	A9(1-90)-HEKMHEGDEG PGAAAKPGHG HGTP

[a] See Table S1 (Supporting Information) for protein nomenclature and Table S2 for protein molecular weights and extinction coefficients.

[b] The “CP-Ser” is routinely omitted in the text for mutants.

[c] Amino acid residues derived from the sequence of murine S100A9 are italicized.

[d] Mutated amino acids are colored red.

[e] HXH motifs are underlined.